Location-resolved PDL Monitoring with Rx-side Digital Signal Processing in Multi-span Optical Transmission System

Motohiko Eto, Kazuyuki Tajima, Setsuo Yoshida, Shoichiro Oda, and Takeshi Hoshida
Fujitsu Limited 1-1 Kamikodanaka 4-Chome, Nakahara-ku, Kawasaki 211-8588, Japan
eto.motohiko@fujitsu.com

Abstract: We propose a novel monitoring that enables to localize PDL in multi-span transmission using only Rx-side DSP and experimentally demonstrate sufficient accuracy within error of 1km with eighty-two polarization combinations in three-span, 180-km transmission line.

1. Introduction

To support diverse optical transmission with different spectral bandwidth in designing and operating optical transport network, optical monitoring technology with cost-effective manner becomes more important than ever, with advanced coherent digital signal processing (DSP) algorithms [1]. Polarization dependent loss (PDL) induced by transmission links and components, e.g., WSS (Wavelength selective switch), is one of the important phenomena that possibly degrades the quality of transmission (QoT). There are several techniques to monitor PDL with coherent DSP [2-4]. However, such approach cannot search for the location of PDL in the link but monitor the amount. Recently power profile estimation (PPE) by receiver (Rx)-side DSP algorithm has been demonstrated [5-7]. In this paper, we propose a novel location-resolved PDL monitoring method by extending the PPE method that we demonstrated previously [5]. The proposed method provides longitudinal power profile of each polarization, thereby identifies the location of PDL in the link. This is helpful to support network operators analyzing a root-cause of QoT degradation in the network. We experimentally evaluated the proposed method applying to dual-polarization signals with eighty-two polarization states in three-span, 180-km transmission link and confirmed sufficient accuracy of PDL location within 1 km.

2. Proposed algorithm for location-resolved PDL monitoring

Fig. 1(a) illustrates the functional block diagram of receiver-side DSP for the proposed location-resolved PDL monitoring. A digital coherent receiver at the end of the link converts received optical signals to the digital data as a set of data for amplitudes and phases for both polarizations. After the conventional demodulation processing, the electromagnetic (EM) fields, E_{sH}, and E_{sV} from carrier phase recovery (CPR), are inputted to the block of the proposed method. These polarizations are rotated to search for the principal axis of PDL [8]. After polarization rotation, the PPE is processed as described in [5]. First, the EM field for each polarization is processed to perform partially chromatic dispersion compensation (CDC), with a value of $n\Delta c$ where Δc is a parameter of the CDC-resolution in the PPE and n is an integer number, i.e., n = 0,1, 2,…, N. This part corresponds to

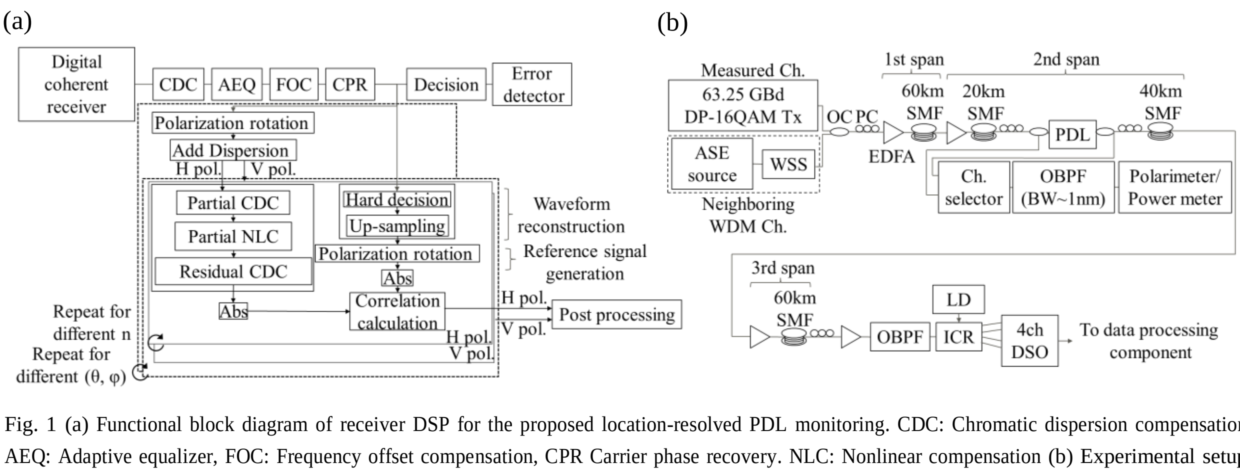

Fig. 1 (a) Functional block diagram of receiver DSP for the proposed location-resolved PDL monitoring. CDC: Chromatic dispersion compensation, AEQ: Adaptive equalizer, FOC: Frequency offset compensation, CPR Carrier phase recovery. NLC: Nonlinear compensation (b) Experimental setup. ASE: Amplified spontaneous emission, WSS: Wavelength selective switch, OC: Optical coupler, PC: Polarization controller, EDFA: Erbium doped fiber amplifier, OBPF: Optical bandpass filter, ICR: Integrated coherent receiver LD: Laser diode, DSO: Digital storage oscilloscope.

fiber back-propagation with distance $n\Delta c/D$, where D is the dispersion of fiber per unit length. Following partial CDC, partial nonlinear compensation (NLC) equalizes a point-wise nonlinear phase noise due to Kerr effect. After partial NLC part, residual CDC is processed. Subsequently, the correlation between the signal and the reference is calculated for a specific polarization angle θ and retardation φ, representing the phase difference between H and V. The reference signal is also reconstructed from CPR output and rotated with the same angle and retardation as in the processing signal. These steps are repeated for different parameters, n, θ and φ. Finally, these results are passed to the post processing to estimate the location of PDL by analyzing difference between profiles for each polarization. The details are explained in the discussion section later.

3. Experimental setup

We experimentally verified the proposed location-resolved PDL monitoring in 180-km-long DWDM transmission line shown in Fig. 1(b) [5]. 63.25-GBaud (GBd) dual-polarization 16-quadrature amplitude modulation (DP-16QAM) signals, and resulting 506-Gbit/s measured signal was pre-distorted with the CD of 1500 ps/nm. Other 34 channels with 50-GHz signals from amplified spontaneous emission (ASE) source and WSS were used as WDM neighboring channels. The WDM signals were launched into 180-km-long straight line consisting of three spans of 60-km-long standard single mode fiber (SSMF) without any in-line dispersion compensation. The fiber launch power was +5 and 0 dBm/channel for measured and neighboring channels, respectively. To emulate PDL, we inserted a 3-dB PDL component at the 80-km point in the transmission link and polarization controllers (PCs) before/after the PDL component. To check polarization states, a polarimeter is connected before/after the PDL component. In case of polarization measurement, it is necessary to switch the polarization from dual polarization to single. After the transmission through three-span transmission link, the signals were received by an integrated coherent receiver with conversion to digitized signals at sampling rate of 80 Gsample/sec. The digital samples were then processed by the proposed PDL monitoring method in offline with a desktop computer.

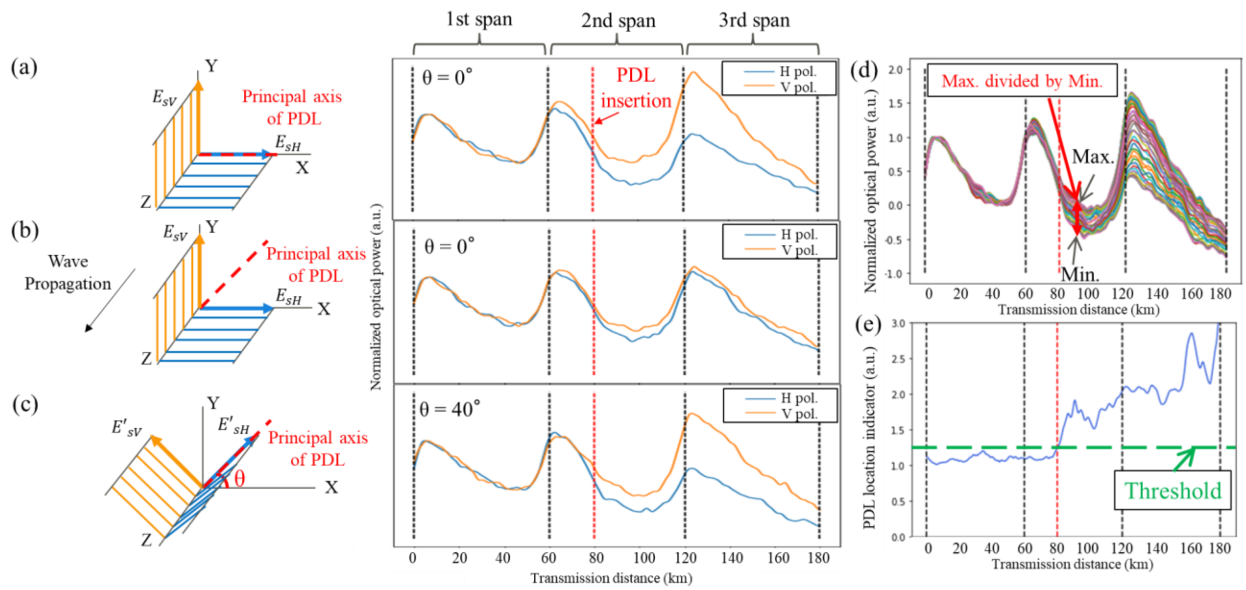

Fig. 2 (a) EM propagation and profile in case that principal axis of PDL is along X axis. (b) In case of different principal axis of PDL before polarization rotation. (c) After polarization rotation processing for (b). (d) Variation of profiles with polarization rotation for H polarization signal. (e) PDL location indicator that is obtained by dividing the maximum value of power profile in (d) by minimum value at each transmission distance.

4. Results and discussion

We investigated the estimation of PDL location with proposed method. The right-hand side of Figs. 2(a), (b) and (c) illustrate the calculated power profiles of H- and V-polarization shown by blue and orange lines, respectively with 50-m step size. The relationship between the polarization state of signal and the principal axis of PDL are schematically illustrated in the left-hand side of Figs. 2(a), (b) and (c), which corresponds to the calculated power profiles. Fig. 2(a) is an example of the case where the principal axis of PDL is along the X axis. In this case, even without polarization rotation, the difference between two power profiles of H- and V-polarization were observed apparently. The two profiles start to separate from the location of PDL component at 80 km indicated by red dot line. However, in Fig. 2(b), as a case of different polarization state that we set the polarization angle to almost 45 degree by adjusting PC in the setup, the two profiles show almost identical, comparing to Fig. 2(a). In this case, it is beneficial to rotate the polarization axis with our proposed method, and the result in Fig. 2(c), obtained by rotating 40 degree, displays the clear difference between two polarizations, which suggests the effectiveness of the proposed method to localize PDL components.

We then describe the post processing for the localization of PDL. From various power profiles in polarization rotations from 0 to 180° shown in Fig. 2(d), we take values that the maximum values divided by the minimum, called to the PDL location indicator, at each transmission distance. This process guarantees to visualize the impact of PDL at each distance accurately, even if the polarization state of signal is changed along the link. As shown in Fig. 2(e), we can identify the location of PDL when the PDL location indicator exceeds the threshold. To verify these processing for the estimation of PDL location, we investigated different polarization states with controlling PCs before/after the PDL component. Fig. 3(a) illustrates twelve different polarization states analyzed before/after PDL by the polarimeter, which are closed to typical polarization states including linear and circular polarizations. These polarization states were slightly different from the actual states at the input into PDL component, due to the change of polarizations in transmission between the PDL component and the polarimeter. We consider this is acceptable to test the polarization dependency of our method for the typical polarizations. Applying above post processing with the threshold at 1.25, the mean value of 78.9 km as the location of PDL suggests its sufficient accuracy of estimation.

To further investigation in various polarization states, we repeated the measurements with randomly setting polarization states including elliptical states, in addition to the data in Fig. 3(a). Fig. 3(b) shows a histogram of PDL locations for eighty-two samples with the same threshold. The estimated PDL location with mean of 79.3 km was agreed well with the actual location of PDL at 80 km in our setup. A slightly larger standard deviation of 3.7 km was obtained. This implies that further investigation on a few outlier data is necessary as a future work. From above results, we experimentally confirmed that the proposed method can localize the PDL under various polarization states within the error of 1 km in this condition.

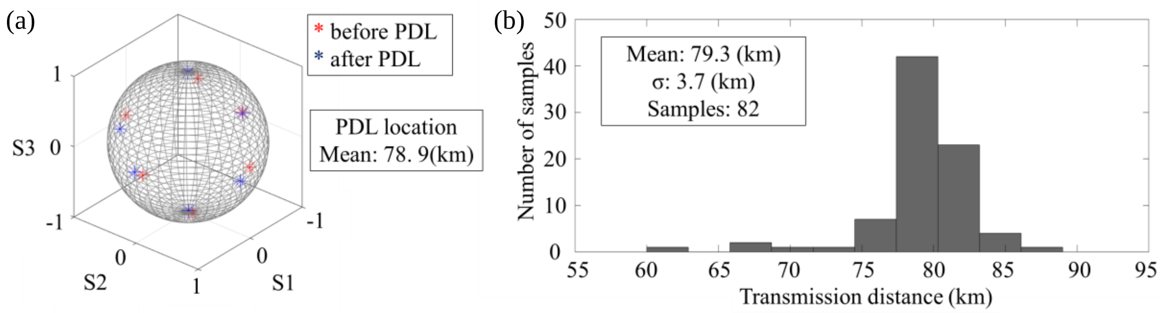

Fig. 3 (a) Polarization states on Poincaré sphere (b) Histogram of estimated location of PDL.

5. Summary

We have developed a location-resolved PDL monitoring method based on our fiber-longitudinal monitor that visualizes distance-wise optical power profile through the entire multi-span link by a coherent receiver. We experimentally measured the PDL locations of eighty-two datasets having different polarization states and confirmed the proposed method can identify the location within the error of 1 km.

Acknowledgement
This work was partly supported by The National Institute of Information and Communications Technology (NICT), Japan, Grant Number 20501.

6. References

[1] T. Hoshida *et al.*, "Advanced DSP for monitoring and mitigation in optical transport networks," OFC 2020, paper Th1I.1, 2020.
[2] G. Huang *et al*., "Polarization Dependent Loss Monitor with Visualization on Poincaré Sphere in Digital Coherent System," ECOC2017, poster P1.SC4.64, 2017.
[3] F. N. Hauske *et al.*, "Optical Performance Monitoring in Digital Coherent Receivers," J. Lightwave Technol., Vol. 27, no. 16, p. 3623 (2009).
[4] C. Xie *et al.*, "Two-Stage Constant Modulus Algorithm Equalizer for Singularity Free Operation and Optical Performance Monitoring in Optical Coherent Receiver," OFC 2010 paper OMK3J, 2010.
[5] T. Tanimura *et al.*, "Advanced data-analysis-based fiber-longitudinal monitoring for optical transport networks," ECOC2020, paper We1H-3, 2020.
[6] T. Sasai *et al.*, "Revealing Raman-amplified power profile and Raman gain spectra with digital backpropagation," OFC 2021, paper M3I.5, 2021.
[7] S. Gleb *et al.*, "Fiber link anomaly detection and estimation based on signal nonlinearity," ECOC2021, paper Tu2C2.5, 2021.
[8] K. Kikuchi, "Fundamental of coherent optical fiber communications," J. Lightwave. Technol., Vol. 34, No. 1, pp. 157-179, 2016.